Exploring the role of homologous recombination deficiency and BRCA1/2 mutations in endometrial cancer

Jonge, M.M. de

Chapter 2

Frequent homologous recombination deficiency in high-grade endometrial carcinomas

Marthe M. de Jonge, Aurélie Auguste, Lise M. van Wijk, Philip C. Schouten, Matty Meijers, Natalja T. ter Haar, Vincent T.H.B.M. Smit, Remi A. Nout, Mark A. Glaire, David N. Church, Harry Vrieling, Bastien Job, Yannick Boursin, Cornelis D. de Kroon, Etienne Rouleau, Alexandra Leary, Maaike P.G. Vreeswijk* and Tjalling Bosse*

***contributed equally**

Clinical Cancer Research 2019 Feb 1;25(3):1087-1097

Abstract

Purpose

The elevated levels of somatic copy number alterations (SCNAs) in a subset of high-risk endometrial cancers are suggestive of defects in pathways governing genome integrity. We sought to assess the prevalence of homologous recombination deficiency (HRD) in endometrial cancers and its association with histopathologic and molecular characteristics.

Experimental Design

Fresh tumor tissue was prospectively collected from 36 endometrial cancers, and functional HRD was examined by the ability of replicating tumor cells to accumulate RAD51 protein at DNA double strand breaks (RAD51 foci) induced by ionizing radiation. Genomic alterations were determined by next generation sequencing and array comparative genomic hybridization/SNP array. The prevalence of *BRCA*-associated genomic scars, a surrogate marker for HRD, was determined in The Cancer Genome Atlas (TCGA) endometrial cancer cohort.

Results

Most endometrial cancers included in the final analysis (n=25) were of non-endometrioid (52%), grade 3 (60%) histology and FIGO-stage I (72%). HRD was observed in 24% (n=6) of cases and was restricted to non-endometrioid endometrial cancers (NEEC), with 46% of NEECs being HRD compared with none of the endometrioid endometrial cancers (EEC, P=0.014). All but 1 of the HRD cases harbored either a pathogenic *BRCA1* variant or high somatic copy number (SCN) losses of HR genes. Analysis of TCGA cases supported these results, with *BRCA*-associated genomic scars present in up to 48% (63/132) of NEEC versus 12% (37/312) of EEC (P<0.001).

Conclusions

HRD occurs in endometrial cancers, and is largely restricted to non-endometrioid, *TP53*-mutant endometrial cancers. Evaluation of HRD may help select patients that could benefit from treatments targeting this defect, including platinum compounds and PARP inhibitors.

Translational relevance

The prognosis for women with high-grade endometrial cancers is poor, with little improvement in the last 2 decades. The mainstay of treatment is surgery (hysterectomy) with or without lymphadenectomy. Although adjuvant radiotherapy is considered standard for high-risk endometrial cancers, the added value of chemotherapy has been subject of recent trials. The randomized PORTEC-3 trial found a significant 5-year failure-free survival benefit (75.5% vs. 68.6%, *P*=0.022) for women with high-risk endometrial cancer treated with adjuvant chemotherapy both during and after radiotherapy versus radiotherapy alone. However, biomarkers predicting chemotherapeutic benefit for patients with endometrial cancers have not been defined to date. In this article, we provide functional evidence that homologous recombination is frequently abrogated in a subset of endometrial cancers, in particularly the "serous-like", *TP53*-mutated subclass which have the worst clinical outcome. Our results suggest that homologous recombination deficiency (HRD) holds promise as a marker to guide treatment decisions in high-risk endometrial cancers, and supports prospective trials investigating agents such as platinum compounds and PARP-inhibitors to target this repair defect in these cancers.

Introduction

Endometrial cancer is the most common gynecologic malignancy in developed countries,[1] with surgery as its primary treatment modality. To guide adjuvant treatment, women with endometrial cancers are stratified according to risk of recurrence using clinicopathologic characteristics.[2, 3] A heterogeneous group of 15%-25% of endometrial cancers are currently considered at high-risk of disease recurrence. This group consists of patients with non-endometrioid endometrial carcinomas [NEEC; uterine serous carcinoma (USC), uterine carcinosarcoma (UCS), clear cell carcinoma (CCC), undifferentiated carcinoma (UC), mixed endometrial cancers], endometrioid endometrial cancers (EEC) grade 3 stage IB-IV and EEC grade 1 and 2 stage II-IV.[2-6] These patients have the poorest clinical outcome, despite optimum adjuvant treatment, which currently comprises a combination of pelvic radiotherapy with or without (platinum-taxane based) chemotherapy.[3-5] In the cohort of Hamilton and colleagues, high-risk EEC grade 3, USC and CCC represented only 28% of the total endometrial cancer cohort but accounted for 74% of endometrial cancer-related deaths,[4] emphasizing the need for better systemic treatments to improve outcomes for these patients.

The Cancer Genome Atlas Research Network (TCGA) analyzed EECs, USCs and mixed carcinomas and identified 4 distinct molecular subclasses based on mutational load and somatic copy number alterations (SCNAs). These 4 subclasses are respectively (i) the *POLE*/ ultramutated, (ii) the microsatellite instability-high (MSI-high)/hypermutated, (iii) the SCNA

low/no specific molecular profile (NSMP), and (iv) the SCNA high (SCNA-hi)/serous-like endometrial cancers (4).[7] Each of these has distinct risk of recurrence and clinical outcome, with *POLE/*ultramutated tumors showing excellent outcome and the SCNA-hi/serous-like subgroup showing the worst prognosis. The first 3 of these subclasses consist mainly of EEC with variants in *PTEN* as the most frequent genetic alteration. In contrast, the SCNA-hi subclass almost exclusively comprises of USC and grade 3 EEC and is strongly associated with pathogenic variants in *TP53*.[7] Interestingly, recent studies demonstrated that rare non-endometrioid subtypes, such as UCS, CCC and dedifferentiated carcinomas appear to be composed of the same 4 molecular subclasses, with UCS being mostly SCNA-hi/*TP53*-mutated and CCC, UC and dedifferentiated endometrial cancers being more heterogeneous.[8-11] The clinical relevance of these observations has increased by the recognition that the TCGA molecular subclasses of endometrial cancers can be recapitulated using pragmatic surrogate markers resulting in subgroups with differing prognoses.[12, 13]

Another interesting observation of the TCGA study were the similarities between the SCNA spectra of the SCNA-hi/*TP53*-mutated endometrial cancers subclass with those of high grade serous ovarian tubal carcinomas (HGSOCs) and basal-like breast cancers.[7, 8] Both HGSOC and basal-like breast cancer are part of the hereditary *BRCA1/2* related breast and ovarian cancer syndrome (HBOC syndrome);[14, 15] characterized by failure of high-fidelity homologous recombination (HR) repair of DNA double-strand breaks (DSBs) mediated by BRCA1 and BRCA2 proteins.[15, 16] Although endometrial cancer is not generally regarded as part of HBOC syndrome, case and cohort studies indicate that serous/serous-like endometrial cancers (including carcinosarcomas) are more prevalent in germline *BRCA1/2* mutation carriers than in the general population.[17, 18] Furthermore, germline alterations in other HR-related genes have been described in patients with endometrial cancer (e.g. *ATM, BARD1, BRIP1, CHEK2, NBN, RAD51C*),[19] raising the question of whether a subset of endometrial cancer is HR-deficient. Shen and colleagues showed that PTEN has a role in the DSB-repair system by regulating the expression of RAD51, a key protein in HR-repair.[20] Given the frequent somatic *PTEN* alterations in endometrial cancers, particularly in MMRd, *POLE* and NSMP-EC, it is conceivable that HR-deficiency might also occur in these subclasses.

There are several methods to determine HR deficiency in tumors. Besides sequencing of genes involved in HR, one can also assess the presence of specific “genomic scars” caused by the use of alternative, error-prone pathways to repair DSBs in the absence of HR. Examples of such alterations that are overrepresented in *BRCA1/2*-null tumors include COSMIC Signature 3 and SCNA profiles associated with widespread loss of heterozygosity (LOH), large-scale state transitions (LST) and telomeric allelic imbalances (TAI).[16, 21-24] A more direct way of testing HR capacity and one which more closely reflects the current status of the tumor, is to determine the ability of tumor cells to perform HR in a functional assay. For this, fresh viable tumor tissue is exposed *ex vivo* to ionizing radiation to induce DNA DSBs. In HR-proficient tumor cells,

RAD51 protein will be recruited to these breaks leading to the formation of RAD51-containing ionizing radiation induced foci (IRIF). In the case of HR-deficient tumor cells, RAD51-IRIF formation will be impaired.[16, 25-27] The RAD51-assay, as a functional read out for HR, has been shown to reliably identify cell lines, xenografts and fresh human tumor tissue with defective HR.[25-28]

The aim of this study was to assess the prevalence of HR deficiency in endometrial cancers using a functional RAD51-IRIF assay, evaluate its association with clinicopathologic characteristics, and define the underlying molecular etiology.

Materials and methods

Patient selection

Fresh endometrial cancer tissue was obtained from patients who underwent surgery at the Leiden University Medical Center (LUMC; Leiden, The Netherlands) between August 2015 and January 2017. All patients with epithelial endometrial cancer (including carcinosarcomas) were eligible for inclusion. After transportation of the surgical specimen to the pathology department, fresh tumor tissue was donated for research if sufficient tumor tissue was available. All cases obtained a unique research number and histotype was assigned by an experienced gynecopathologist (T. Bosse). The local medical ethics committee approved the study protocol (B16.019) and specimens were handled according to the "Code for Proper Secondary Use of Human Tissue in the Netherlands" (Dutch Federation of Medical Scientific Societies).

Functional *ex vivo* RAD51 assay to determine HR capacity

Fresh endometrial cancer tissue samples were kept at 4°C in OSE Culture Medium (Wisent Bioproducts, cat. 316-030-CL) supplemented with 10% FBS and 1% penicillin-streptomycine (100 U/ml). Tissue was manually cut in 5-mm slices and after an incubation period of at least 4 hours at 37°C, the slice was irradiated with 5-Gy ionizing radiation (200 kV, 4mA, YXLON Y.TU 225-D02) to induce DNA DSBs. Samples were then incubated on a rotating device (60 rpm) for two hours at 37°C in the OSE culture medium supplemented with 5-Ethynyl-2'-deoxyuridine (EdU) to a final concentration of 20 µmol/L (Component A; catalog No. C10340, Click-iT EdU Imaging Kits, Invitrogen) according to manufacturer's instructions. After incubation, tissue slices were fixed in formalin (4%) and embedded in paraffin. Leftover endometrial cancer tissue was stored in liquid nitrogen in Recovery Cell Culture Freezing Medium (Sigma, catalog No. 12648010) to ensure viability after cryostorage.

Immunofluorescent staining. After irradiation and incubation, tumor samples were costained for RAD51, Geminin and EdU using anti-RAD51 (GTX70230, GeneTex), anti-geminin (10802-1-

AP, Protein Tech group), and the Click-iT reaction cocktail for EdU detection. For details, see Supplementary Materials and Methods.

Quality control and scoring of the RAD51-assay. To ensure high-quality data, we applied 3 stringent inclusion criteria. First, a semiquantitative analysis of the quality of the tumor tissue was performed on a hematoxylin and eosin (H&E)-stained serial section of the irradiated tumor slice used for the RAD51-IRIF assay. The tissue quality was scored (score 1-2=poor, 3-4=moderate, 5-6=good) based on the sum of the tissue vitality (1=poor, 2=moderate, 3=good) and tumor percentage (0=<5%, 1=5%-20% 2=20%-49% 3=≥50%). Samples were excluded when the total tissue quality score was 2 or less, or when the tumor percentage was <5%. Second, we only included samples for which we were able to score RAD51-IRIF in at least 50 geminin positive cells, defined by complete nuclear staining. Geminin is a cell-cycle marker to identify cells in the S/G_2-phase, the cell cycle phases in which HR is active. Third, >30% of the geminin positive cells had to be EdU positive. EdU is a nucleoside analogue that is actively incorporated into the DNA during DNA synthesis.[29] Absence or low levels of EdU incorporation are indicative for limited DNA replication capacity of the tumor cells. As nonproliferative cells are not able to perform HR, this criterion avoids incorrect classification of tumors as HR-deficient.

When 1 of these 3 criteria was not met, cryopreserved tissue from the same tumor was thawed, irradiated, and analyzed. If this "back-up" sample also failed to meet all the quality controls, the tumor sample was excluded from further analysis.

For scoring, we used preestablished cut-off values.[25] A tumor was considered HR-proficient when more than 5 RAD51-IRIF per nucleus were present in >50% of geminin positive cells and HR-deficient when ≤20% of geminin-positive tumor cells formed RAD51-IRIF after ionizing radiation (Fig. 1). RAD51-IRIF formation in 21%-50% geminin-positive tumor cells was considered HR-intermediate. All cases were scored for Geminin, RAD51, and EdU by 2 independent observers via immunofluorescence microscopy and the average score was used for the category assignment.

Genetic and epigenetic analyses

DNA isolation. Tumor DNA was isolated from formalin-fixed paraffin-embedded (FFPE) tissue blocks either by taking 3 0.6-mm tumor cores or by microdissection of tumor areas (10-µm slides). DNA isolation was performed fully automated using the Tissue Preparation System (Siemens Healthcare Diagnostics) as described previously.[30] In addition, for a subset of cases, high-quality tumor DNA was isolated from frozen tumor tissue using 5-10 whole cryosections (20 µm) and the Wizard Genomic DNA purification KIT (Promega) according to manufacturer's protocol. An H&E cryoslide (5 µm) was made to determine tumor percentage.

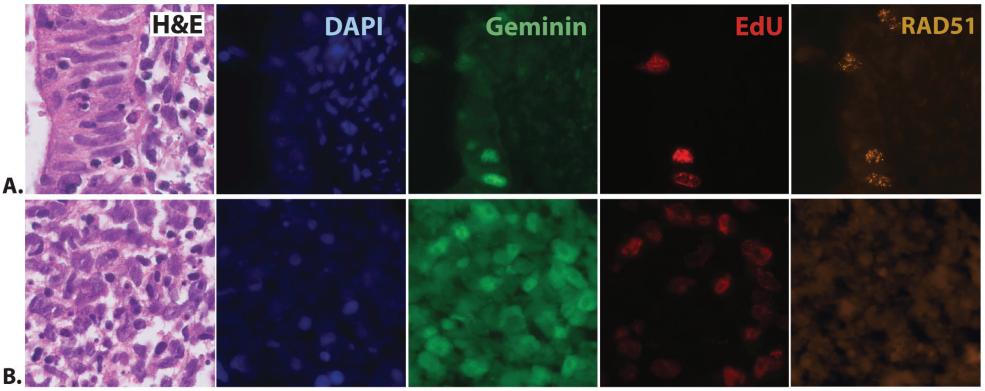

Figure 1: Functional Ex Vivo RAD51 assay to determine homologous recombination repair capacity in endometrial cancer. A, Example of a homologous recombination repair proficient endometrioid endometrial carcinoma (case 26). In the H&E, the presence of tumor tissue is confirmed. Cell nuclei are stained with DAPI. Geminin-staining marks cells in S- and G_2-phase. RAD51 foci can be visualized in geminin-positive tumor cells 2 hours after *ex vivo* exposure to X-rays (5 Gy). **B,** Example of a homologous recombination repair-deficient carcinosarcoma (case 13). After *ex vivo* treatment with ionizing radiation, only 2% of the geminin-positive cells demonstrates accumulation of RAD51-foci.

The Qubit dsDNA HS Assay Kit was used for DNA quantification according to manufacturer's instructions (Qubit 2.0 Fluorometer, Life Technologies).

aCGH / SNP array to determine SCNAs. SCNAs were determined using either the Agilent SurePrint G3 CGH Microarray (8 x 60k probes, Agilent technologies) on 300-ng DNA derived from frozen tumor tissue (*n*=16, Case ID; 1, 3, 6, 7, 9, 12, 13, 14, 15, 16, 17, 18, 19, 21, 22, 24) or the OncoScan™ FFPE Assay Kit (335k probes, Thermo Fisher Scientific) on 80-ng FFPE-isolated DNA (*n*=9, Case-ID; 20, 25, 26, 27, 29, 32, 33, 34, 36). Prior paired analysis of ten ovarian tumor samples showed that the SCNA were similar independently of the platform used (Supplementary Fig. S1). Furthermore, unsupervised Pearson hierarchical clustering performed on the included tumor samples demonstrated a natural division between samples independent of the platform used (Supplementary Fig. S2). For both platforms, samples were included when the tumor cell percentage was at least 30%. The mean tumor cell percentage of the DNA derived from frozen tumor tissue samples included for the aCGH was 78% (range: 30%-95%). The mean tumor cell percentage of the FFPE tissue-isolated DNA samples for the SNP array was 71% (range: 50%-90%). Analysis was performed according to manufacturer's instructions. Microarray data is available upon request. For details, see Supplementary Materials and Methods.

Genomic instability score. The genomic instability score (GIS) was calculated as the number of altered segments superior to 15 Mbp and inferior to chromosome arm, and samples were classified in 3 categories using an unsupervised machine learning (kmeans – python scikit)

based on GIS. For details on the analysis, see Supplementary Materials and Methods. The 3 categories were SCNA-low, SCNA-high and SCNA-extremely high.

Somatic copy-number losses. As a marker for potential loss of function of HR genes, the presence of "high somatic copy-number (SCN) losses" was determined for all cases by using a very stringent cut-off value; $\log_2$ratio ≤-0.7. This stringent cut-off value was used to select for SCN losses in genes that are more likely clonal and/or homozygous. The same cutoff was applied for both platforms (CGH Agilent and Oncoscan) as both yield similar results. HR genes were defined according to a previously published list by Riaz and collegues; HR-genes were categorized as either "core" HR genes (involved in the core HR machinery) or "related" HR genes (involved in closely related processes).[31]

Next generation sequencing. Next-generation sequencing (NGS) was performed using FFPE-isolated tumor DNA with a total input of 500-1,000 ng per sample. The mean tumor cell percentage of the included samples was 68% (range: 30%-90%). An Agilent Sureselect$^{XT\ HS}$ Custom panel made in SureDesign (Agilent technologies) was used for variant detection with the following HR-genes design: *ATM*; exons 2-63, *BARD1*; exons 1-10, *BRCA1*; exons 1-24, *BRCA2*; exons 2-27, *BRIP1*; exons 2-20, *CDK12;* exons 1-14, *CHEK2*; exons 2-15, *PALB2*; exons 1-13, *RAD51C*; exons 1-9, *RAD51D*; exons 1-14. Additional genes included in the panel were *TP53 (*exons 1-12) and *CCNE1* (only for amplification detection). For details on the data analysis, see Supplementary Materials and Methods.

Variants were categorized using the 5-tier pathogenicity classification according to Plon and colleagues, 2008; class 1=benign, class 2=likely benign, class 3=variant of unknown significance (VUS), class 4=likely pathogenic, class 5=pathogenic.[32] Only class 3, 4 and 5 variants are reported in the manuscript. Variants were annotated based on the basis of build GRCH37 (hg19) using the following transcript numbers: *ATM;* NM*_000051.3, BRCA1;* NM_007294.3*, BRCA2;* NM_000059.3*, BRIP1; NM_032043.2,CHEK2;* NM_007194.3*, CDK12;* NM_016507.3, *RAD51D;* NM_002878.3.

BRCA1 hypermethylation using MS-MLPA. The presence of *BRCA1* promotor hypermethylation was assessed for all cases using tumor DNA isolated from FFPE-tissue. For this, the SALSA MLPA ME001 tumor suppressor mix (MRC-Holland) was used as described in the Supplementary Materials and Methods.

IHC analysis. If not yet performed in routine diagnostics (Autostainer Link 48, DAKO), additional IHC stainings for PMS2 (Clone EP51, 1:25, DAKO), MSH6 (Clone EPR3945, 1:400, GeneTex), PTEN (Clone 6H2.1, 1:200, DAKO), MRE11 (clone 31H4, 1:400, Cell Signalling Technology) and BAP1 (clone C4, 1:100, Santa Cruz Biotechnology) were performed on whole slides (4 µm) as described in the Supplementary Material and Methods.

POLE sequencing. Unidirectional Sanger sequencing was performed to screen exons 9 (forward), 13 (reverse) and 14 (reverse) for somatic *POLE* exonuclease domain mutations as described previously using FFPE tumor DNA.[33] To sequence exon 14, the following primers were used; forward: 5'- tctggcgttctctcctcag-3', reverse: 5'- cgacaggacagataatgctcac-3'. Mutations were confirmed by Sanger sequencing in the opposite direction. *POLE* transcript NM_006231.3 was used for variant annotation.

TCGA classification based on surrogate markers. All endometrial cancers included in this study were classified according to the previously described molecular subclasses using a surrogate marker approach. For details, see Supplementary Materials and Methods.

BRCA-associated genomic scars in the TCGA cohort

To determine the presence of *BRCA*-associated genomic scars in the TCGA-EC cohort, SCNA data and somatic mutation annotation files (MAF) were obtained from Firebrowse (http://firebrowse.org/) using data version 2016_01_28; doi:10.7908/C11G0KM9.[34] First, we assessed the presence of specific patterns of somatic copy-number gains and losses that have previously been linked to *BRCA1* or *BRCA2* mutated breast and ovarian cancer to classify tumors in *BRCA*-like or non-*BRCA*-like.[35] Second, we assessed the number of LST (cut-off used to define HR-deficiency ≥15), the presence of COSMIC signature 3 and the presence of biallelic pathogenic mutations in 102 HR genes as defined by Riaz and colleagues.[31] For details regarding these analyses, see Supplementary Materials and Methods.

Statistical analysis

Comparison of age between groups was performed using the unpaired *t* test. Associations between all categorical variables were tested using a 2-sided Fisher exact test. A *P* value of <0,05 was considered significant. Cohen's kappa coefficient (κ) was used to measure interobserver and intertest agreement. IBM SPSS version 23.0 (SPSS, Inc., Chicago, USA) and R (http://r-project.org) were used for statistical analysis.

Results

Homologous recombination repair deficiency and clinicopathologic characteristics

Fresh tumor tissue was prospectively obtained from 36 patients. Twenty-five samples (12 EEC and 13 NEEC) passed our stringent quality controls and were included for further analyses (Fig. 2). Clinicopathologic characteristics of the total cohort are described in Supplementary Table S1. The percentage of Geminin$^+$/RAD51$^+$ cells scored after *ex vivo* exposure to ionizing radiation by the 2 independent observers was comparable, with a median score difference

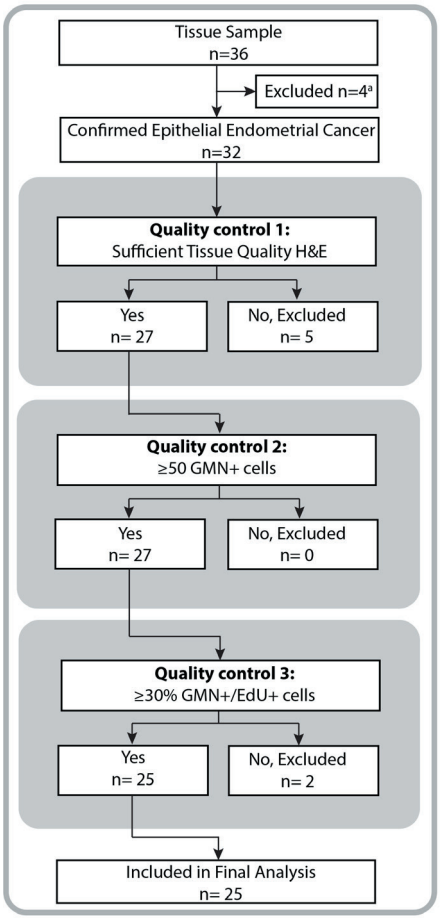

Figure 2: Flowchart illustrating the selection of cases for analysis. Of 36 samples, four[a] cases were excluded because histological evaluation demonstrated no epithelial endometrial malignancy (2x cervical carcinoma, 1x leiomyosarcoma, 1x benign). Tissue was thawed and reanalysed for 10 cases because they did not pass 1 of the quality controls (QC1; *n*=5, QC2; *n*=0, QC3; *n*=5). For 3 cases (all initially excluded during QC3), this procedure resulted in sufficient quality improvement to allow inclusion for final analysis. For 1 case, only frozen tissue was available, which was of sufficient quality. In total, 25 cases passed all quality controls.

within cases of 6% (range: 0%-41%). Interrogator reliability for final HR category assignment was high (κ=0.85).

In total, 6 (24%) endometrial cancers were classified as HR-deficient, 17 (68%) as HR-proficient and 2 (8%) as HR-intermediate. Clinicopathologic characteristics of groups stratified by HR status are shown in Table 1 and Fig. 3A. HR-intermediate cases are described in Supplementary Table S2. HR deficiency was significantly associated with non-endometrioid histology; all 6 (100%) HR-deficient tumors were NEEC, compared with none of 12 EEC tested (*P*=0.014). The 6 HR-deficient NEEC were either USC (*n*=3, 50%) or UCS with serous epithelial

component (*n*=3, 50%). The 17 HR-proficient tumors were histologically more diverse; 11 (65%) EEC, 2 (12%) CCC, 2 (12%) dedifferentiated carcinomas, 1 (6%) USC and 1 (6%) UCS with serous epithelial component. When only considering USC and UCS (both with serous and endometrioid epithelial component), 6 of 9 tumors (67%) were HR-deficient.

HR-deficient endometrial cancers were more often high grade (grade 3; 100%) compared to HR-proficient endometrial cancers (41%, *P*=0.019), reflecting the non-endometrioid histology in the HR-deficient group. HR-deficient endometrial cancers presented more often in a high FIGO-stage compared to HR-proficient endometrial cancers (I vs III/IV; *P* =0.021) and had more frequent lymphovascular space involvement (*P*=0.045). We did not observe an association between HR-deficiency and loss of PTEN expression by IHC, with 1 (17%) of the HR-deficient cases showing PTEN loss compared with 47% of HR-proficient cases (*P*=0.340). There was also no association between HR capacity and age of endometrial cancer diagnosis (*P*=0.431). *TP53* variants were more often present in HR-deficient tumors (100%) compared with HR-proficient tumors (41%; *P*=0.019). In total, 46% of the *TP53*-mutated endometrial cancers were HR-deficient.

Two cases were assigned HR-intermediate. One was a grade 3 EEC that was just above the threshold of being HR-deficient (case 27; Geminin$^+$/RAD51$^+$; 23%). The other case was a UCS with an endometrioid epithelial component (case 18; Geminin$^+$/RAD51$^+$; 44%, Fig. 3A and Supplementary Table S2).

Homologous recombination repair capacity and molecular subgroups

Surrogate markers were used to classify the endometrial cancers into the 4 molecular subgroups as defined by the TCGA study (Table 1; Fig. 3A). HR-deficient endometrial cancers were significantly more often classified as SCNA-hi/*TP53*-mutated compared to HR-proficient endometrial cancers, with all HR-deficient endometrial cancers being SCNA-hi/*TP53*-mutated compared with 6 (35%) of the HR-proficient endometrial cancers (*P*=0.014). The HR-proficient group was heterogeneous with all molecular subgroups represented; 9 (53%) NSMP, 6 (35%) SCNA-hi/*TP53*-mutated, 1 (6%) *POLE*/ultramutated and one (6%) MMRd/hypermutated.

To further characterize our cohort, we performed SCNA analyses using a genomic instability score (GIS) based on the number of altered segments greater than 15 Mbp and smaller than a whole chromosome arm. For this, samples were classified in 3 categories using unsupervised machine learning (k-means clustering); SCNA-low, SCNA-high and SCNA-extremely high. All HR-deficient endometrial cancers (100%) were either SCNA-high (*n*=2) or SCNA-extremely high (*n*=4), compared with 7 (41%; 6 SCNA-high, 1 SCNA-extremely high) of the HR-proficient endometrial cancers (*P*=0.019, Fig. 3A and Table 1). An association was observed between the SCNA status and the presence of a *TP53* variant, with *TP53* variants being significantly

Table 1. Clinicopathological characteristics stratified for homologous recombination capacity

	HR deficient ***n*** **(%)**	**HR proficient** ***n*** **(%)**	***P*** **value**
Total	6 (100)	17 (100)	
Age, years			
Mean ±SD	70 ±9.3	66 ±10.6	0.431
Tumor			
Primary	6 (100)	17 (100)	
Recurrent	0 (0)	0 (0)	
Histologic subtype			
Endometrioid	0 (0)	11 (65)	**0.014**[a]
Non-endometrioid	6 (100)	6 (35)	
Serous	*3 (50)*	*1 (6)*	
Carcinosarcoma	*3 (50)*	*1 (6)*	
Clear cell	*0 (0)*	*2 (12)*	
Dedifferentiated	*0 (0)*	*2 (12)*	
Histologic grade			
1+2	0 (0)	10 (59)	**0.019**
3	6 (100)	7 (41)	
FIGO 2009			
I	2 (33)	15 (88)	**0.021**
III/IV	4 (67)	2 (12)	
Adnexal involvement			
yes	1 (17)	2 (12)	1.00
no	5 (83)	15 (88)	
LVSI			
yes	4 (67)	3 (18)	**0.045**
no	2 (33)	14 (82)	
PTEN-IHC			
loss of expression	1 (17)	8 (47)	0.340
normal expression	5 (83)	9 (53)	
aCGH			
Copy number extremely high	4 (67)	1 (6)	**0.019**[b]
Copy number high	2 (33)	6 (35)	
Copy number low	0 (0)	10 (60)	
TP53			
Mutation	6 (100)	7 (41)	**0.019**
No mutation	0 (0)	10 (59)	
TCGA subgroups			
TP53	6 (100)	6 (35)	**0.014**
NSMP/POLE/MMRd	0 (0)	11 (65)	

NOTE: Bolded *P* values are considered significant (*P*<0.05*)*. *P* values were calculated using the 2-sided Fisher exact test for the categorical variables and the unpaired *t* test for the difference in age.
Abbreviations: LVSI, lymphovascular space involvement; MMRd, mismatch repair deficient; NSMP, no specific molecular profile.
[a]Endometrioid versus non-endometrioid histology was compared.
[b]Copy number extremely high + copy number high versus copy number low was compared.

more common in SCNA-high or extremely high endometrial cancers (79%; 11/14) compared with SCNA-low endometrial cancers (18%; 2/11, *P*=0.005).

Genetic alterations in HR genes and relation to HR phenotype

We performed (epi)genetic analysis to identify possible loss-of-function alterations that could explain the HR deficiency. This included NGS (variants HR genes), aCGH/SNP array (high SCN losses of HR genes; $\log_2$Ratio≤-0.7), MS-MLPA (*BRCA1* promoter hypermethylation) and immunohistochemistry (MRE11, BAP1).

In 2 out of 6 HR-deficient endometrial cancers the presence of a pathogenic *BRCA1* variant with LOH of the wild-type allele could explain the HR-deficient phenotype (case 9; *BRCA1,* c.4327C>T, p.Arg1443*, and case 15; *BRCA1,* c.3013delG, p.Glu1005fs, see Fig. 3B and Supplementary Table S3). Two other HR-deficient cases harbored a VUS in an HR gene; case 36; *RAD51D,* c.433C>T, p.Arg145Cys and case 19; *ATM*, c.6543G>T, p.Glu2181Asp. As it is uncertain whether these variants will affect protein function and the variant allele frequency (VAF) was low (32%, and 34%, respectively) with tumor percentages of 75% and 70%, respectively, it is unlikely that these variants were causative for the observed HR deficiency.

High SCN losses in HR core and HR-related genes were observed for both cases in which no variants were identified (cases 12 and 13) and for case 19 in which a VUS in *ATM* was detected (Figs. 3B and 4). Case 36, in which a *RAD51D* VUS was identified, did not show SCN losses in HR genes with a $\log_2$ratio of ≤-0.7. None of the included cases demonstrated *BRCA1* promoter hypermethylation or IHC BAP1 or MRE11 expression loss.

In the HR-proficient endometrial cancers, variants in HR genes were present in 2 cases (Fig. 3B). Case 26, the *POLE*-mutated tumor, harbored a class 5 *CHEK2* variant c.1510G>T, p.Glu504* (VAF: 28%) that likely occurred as a consequence of the *POLE* mutation as it is concordant with the known mutational bias it causes.[36] Case 23, the MMRd endometrial cancer, harboured 4 *ATM* variants. One of the 4 *ATM* variants was a class 5 variant; c.640delT, p.Ser214fs, VAF: 5.5%, and the remaining 3 were all VUS (Supplementary Table S3). None of the HR-proficient endometrial cancers demonstrated high SCN losses of the HR core genes. Cases 01 and 34 did show high SCN losses in HR-related genes (Figs. 3B and 4).

Two endometrial cancers demonstrated an HR-intermediate phenotype (Fig. 3A and B; Supplementary Table S2). Case 27 harbored 2 *BRCA2*, 1 *BRIP1* and 1 *CDK12* variant. The *BRCA2* variant with the highest VAF (64%) was a duplication of an adenine; c.6373dupA, p.Thr2125fs. In addition, an in-frame deletion (c.6306_6413del, p.Ser2103_Val2138del) spanning the frameshift variant was present with a VAF of 28%, likely restoring the BRCA2 function in a subset of the tumor cells. Case 18 harbored a class 5 *BRIP1* variant; c.632delC,

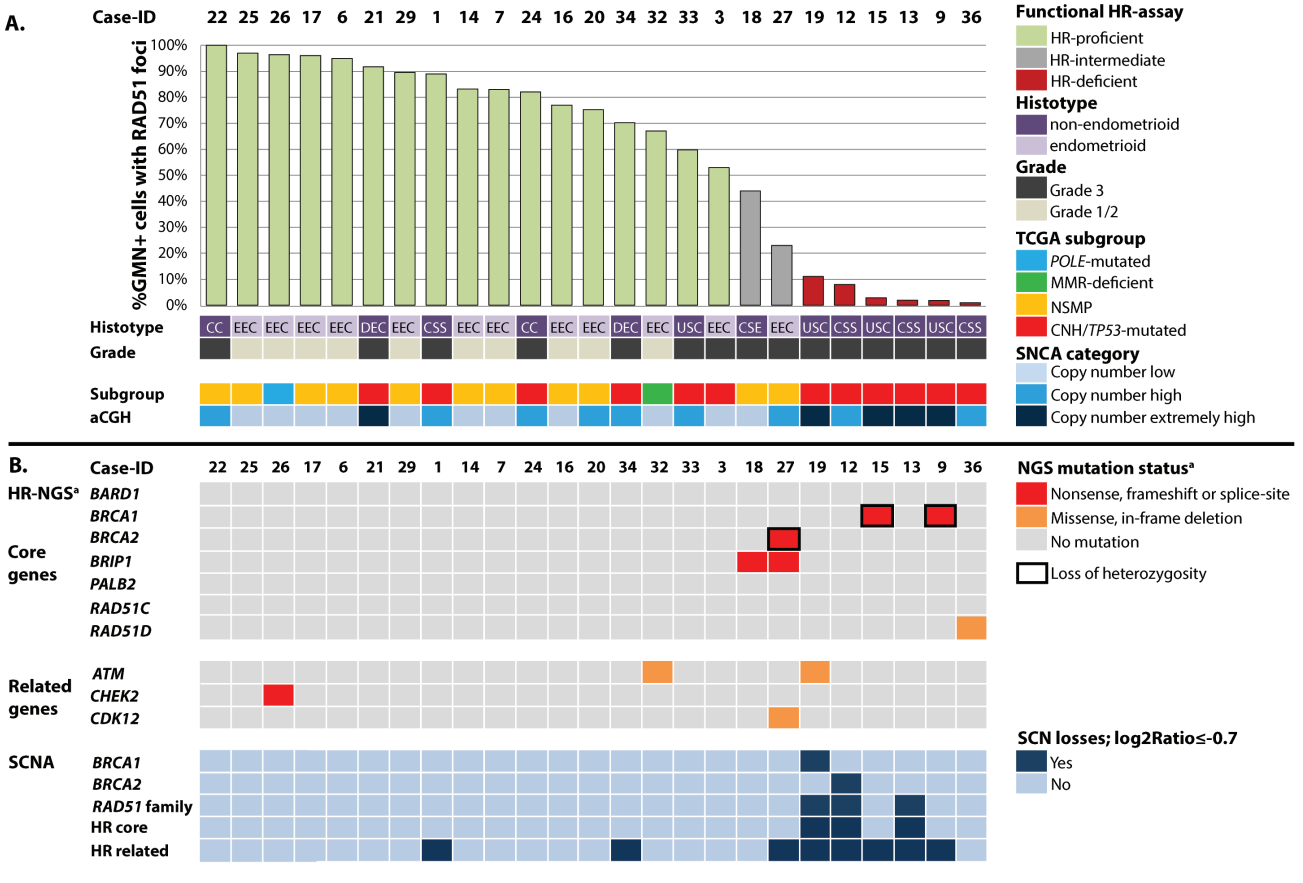
A.
Case-ID
22 25 26 17 6 21 29 1 14 7 24 16 20 34 32 33 3 18 27 19 12 15 13 9 36
%GMN+ cells with RAD51 foci
100%
90%
80%
70%
60%
50%
40%
30%
20%
10%
0%
Histotype
CC EEC EEC EEC EEC DEC EEC CSS EEC EEC CC EEC EEC DEC EEC USC EEC CSE EEC USC CSS USC CSS USC CSS
Grade
Subgroup
aCGH
Functional HR-assay
HR-proficient
HR-intermediate
HR-deficient
Histotype
non-endometrioid
endometrioid
Grade
Grade 3
Grade 1/2
TCGA subgroup
POLE-mutated
MMR-deficient
NSMP
CNH/TP53-mutated
SNCA category
Copy number low
Copy number high
Copy number extremely high
B.
Case-ID
22 25 26 17 6 21 29 1 14 7 24 16 20 34 32 33 3 18 27 19 12 15 13 9 36
HR-NGS[a]
Core genes
BARD1
BRCA1
BRCA2
BRIP1
PALB2
RAD51C
RAD51D
Related genes
ATM
CHEK2
CDK12
SCNA
BRCA1
BRCA2
RAD51 family
HR core
HR related
NGS mutation status[a]
Nonsense, frameshift or splice-site
Missense, in-frame deletion
No mutation
Loss of heterozygosity
SCN losses; log2Ratio≤-0.7
Yes
No

< Figure 3: Tumor characteristics (A) and genetic changes (B) stratified for homologous recombination capacity. Each column represents one case. **A**, Cases were classified in TCGA subgroups using surrogate markers as described in the Supplementary Material and Methods. Case 26 contained a *POLE* variant and a *TP53* variant and was classified in the *POLE*-mutated subgroup. Case 09 demonstrated subclonal loss of PMS2 with normal expression in the tumor tissue on which the RAD51 assay was performed, together with a *TP53* variant, and was classified as *TP53* mutant. **B,** HR genes were categorized as either being involved in the core process of HR ("core" genes) or being involved in related processes to HR ("related" genes), as previously described by Riaz and collegues.[31] Abbreviations: CC: Clear Cell Carcinoma, CSE: CarcinoSarcoma with Endometrioid epithelial component, CSS: CarcinoSarcoma with Serous epithelial component, DEC: Dedifferentiated Endometrial Carcinoma, EEC: Endometrioid Endometrial Carcinoma, HR: Homologous Recombination, USC: Uterine Serous Carcinoma. [a]Only variants with a variant allele frequency of ≥25% are shown. When multiple variants were present in the same gene, the most pathogenic variant is shown.

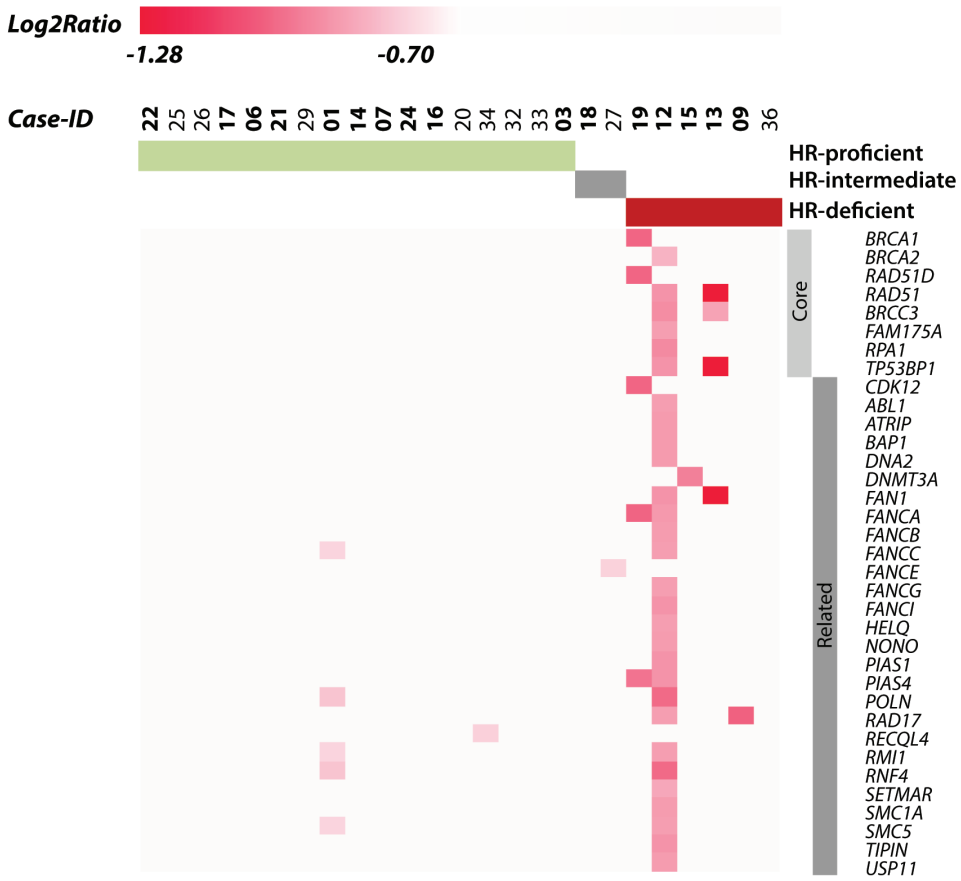

Figure 4: Somatic copy-number losses stratified for homologous recombination (HR) capacity. HR genes were selected and divided in HR-core or HR-related genes as described by Riaz and colleagues.[31] Only those genes with SCN losses of $\log_2$ratio≤-0.7 in at least 1 of the included cases are visualised. Data were extracted from the aCGH data as described in the Supplementary Materials. Bolded cases were analysed using the CGH Agilent platform, others were analysed using the Oncoscan platform.

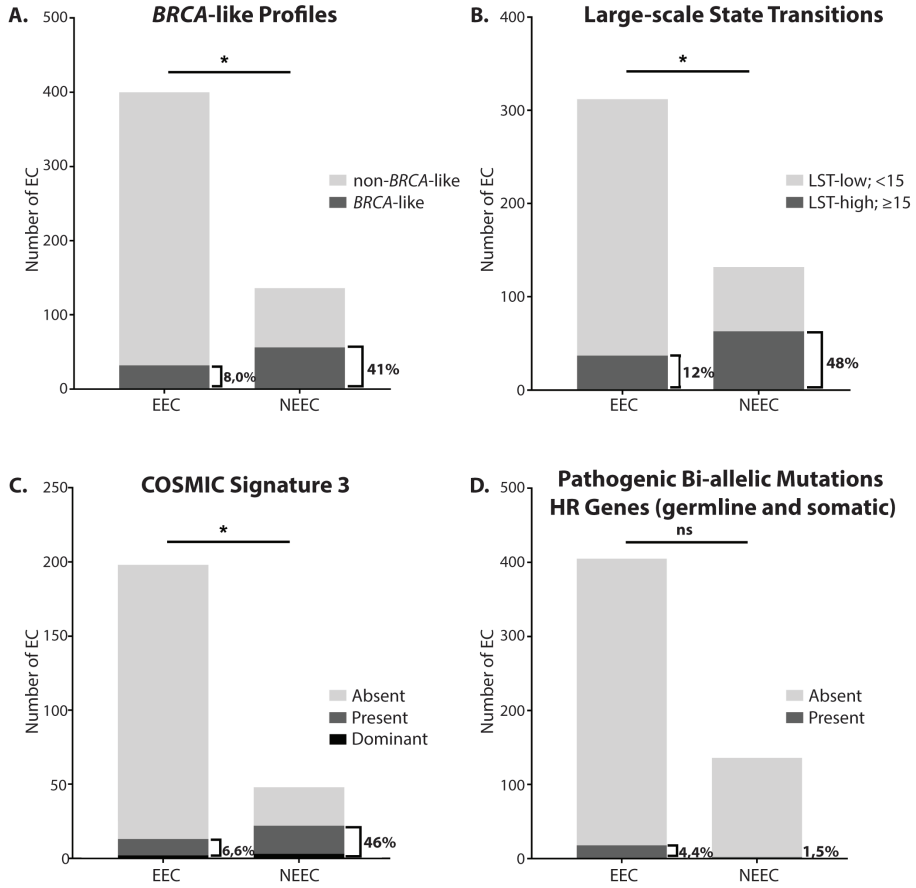

Figure 5: *BRCA*-associated genomic scars as surrogate marker for HR deficiency in the TCGA-endometrial cancer cohort. A, A *BRCA*-like profile was present in 32/400 of EECs and 56/136 of NEECs. **B,** A high LST score (≥15) was present in 37/312 of EECs and 63/132 of NEECs. **C,** COSMIC signature 3 was present in 13/198 of EECs and 22/48 of NEECs, and it was present as dominant signature in 2/198 of EECs and 3/48 of NEECs. **D,** Pathogenic biallelic mutations in HR genes were present in 18/405 of EECs and 2/136 of NEECs. The intertest agreement (accuracy and Cohen's kappa coefficient respectively) were as follows; 0.82 and 0.46 for LST versus *BRCA*-like profiles, 0.84 and 0.40 for LST versus signature 3, 0.85 and 0.36 for *BRCA*-like profiles versus signature 3. (ns, not significant; *,P<0.001).

p.Pro211fs with a VAF of 28%. None of the HR-intermediate cases demonstrated high SCN losses in the HR core genes. Case 27 did show SCN losses in 1 HR-related gene (Figs. 3B and 4).

BRCA-associated genomic scars in the TCGA cohort

To validate the occurrence of HR deficiency in an additional endometrial cancer cohort, we used SCNA data and somatic MAFs from the TCGA study to determine the presence of *BRCA*-like profiles (data available for *n*=536), LSTs (data available for *n*=444), COSMIC signature 3 (data available for *n*=246) and pathogenic biallelic alterations in HR genes (data

available for *n*=541). Because our data showed a clear difference in the presence of HR-deficiency between EEC and NEEC, we stratified the cohort by histotype (EEC vs NEEC, the latter including both mixed-endometrial cancers and USC). Both a *BRCA*-like profile and a high LST score were significantly more common in NEEC (*BRCA*-like profile, 41.2%; LST, 47,7%) compared with the EEC (*BRCA*-like profile, 8.0%; LST, 11.9%), *P*<0.001 (Fig. 5A and B). COSMIC signature 3 was present in 6.6% of EEC and 45.8% of NEEC (*P*<0.001, Fig. 5C). It was present as dominant signature in 1.0% (*n*=2) of EEC and 6.3% of NEEC (*n*=3, *P*=0.052). Somatic or germline pathogenic biallelic variants in HR pathway genes were present in 4.4% of EEC and in 1.5% NEEC (*P*=0.19, Fig. 5D). The high prevalence of *BRCA*-associated genomic scars in the TCGA-endometrial cancer cohort supports that HR deficiency occurs in endometrial cancers, especially in NEEC, as observed in our prospective cohort.

Discussion

Using a functional assay to assess homologous recombination repair capacity, we found that HR deficiency is common in endometrial cancers, especially in NEEC (46%). The observation that all HR-deficient endometrial cancers were *TP53*-mutated and of USC or UCS histology (comprising 67% of the included USC/UCS), further extends the established parallels between a subset of endometrial cancer and HGSOC. In 5 of 6 HR-deficient tumors, we identified alterations in core HR genes (2 cases with a pathogenic variant in *BRCA1* and 3 cases with high SCN losses of HR core genes). Independent validation using the TCGA endometrial cancer cases in which we determined the prevalence of *BRCA*-associated genomic scars underscored the high prevalence of HR deficiency in NEEC.

Using established cut-off values to assign endometrial cancers to different HR categories, we were able to assign 23 of 25 endometrial cancers into either the HR-deficient or HR-proficient category, leaving 2 cases in the HR-intermediate category (cases 27 and 18). Case 27 was a second recurrence of a *TP53* wild-type grade 3 EEC after 2 previous lines of platinum-based chemotherapy. At initial treatment there was a partial response (according to the RECIST criteria) after 3 courses of neoadjuvant carboplatin/paclitaxel. Genomic analysis identified 2 *BRCA2* variants; 1 truncating frameshift variant and 1 in-frame deletion, spanning the region containing the frameshift variant. It is likely that the in-frame deletion is a secondary somatic variant (partially) restoring the BRCA2 function, a scenario described previously.[37] This is a relevant observation, as it suggests that *TP53* wild-type endometrial cancers with endometrioid histology may also be HR-deficient.

PTEN alterations are frequent in endometrial cancers, particularly in EEC and may modulate DSB-repair capacity by regulating the expression of RAD51.[20] *In vitro* studies have shown contradictory results, with some reporting no correlation between PTEN loss and HR-

deficiency,[38, 39] whereas others did find a correlation.[40] In our study, we did not observe a correlation between HR capacity and IHC PTEN expression.

On the basis of the high prevalence of HR-deficiency in our cohort, one might speculate that a proportion of, especially the serous/serous-like endometrial cancers would be responsive to platinum-based chemotherapy.[41, 42] The PORTEC-3 trial suggested that the addition of platinum/taxane-based chemotherapy to radiotherapy in patients with USC resulted in a similar failure-free survival benefit as for the overall cohort of patients with high-risk endometrial cancers, although this benefit was not significant.[43] Furthermore, a grouped analysis among 1,203 patients with advanced or recurrent endometrial cancers participating in 4 Gynecologic Oncology Group (GOG) trials found similar overall response rates to chemotherapy for USC as for other histotypes (EEC, CCC).[44] In contrast, the pooled analysis of the NSGO-EC-9501/EORTC-55991 trials showed a significant progression-free survival benefit of the addition of adjuvant (platinum-based) chemotherapy for EEC but not patients with USC and CCC.[45] Possible explanations for these different trial outcomes may be the small number of included USC, the different chemotherapy combinations used within trials (apart from PORTEC-3) and finally, the major difficulties pathologist are having with assigning histotype, particularly in high-grade endometrial cancers.[46] For these reasons, future endometrial cancer trial-designs in which (platinum-based) chemotherapy is included, should consider HR status as a biomarker for treatment stratification.

Multiple studies have already shown that PARP-inhibitors improve progression-free survival in patients with platinum sensitive recurrent ovarian cancer.[47-49] Although most treatment benefit is observed for *BRCA1/2*-mutated tumors, an increased beneficial effect could also be observed for tumors with genetic alterations that are suggestive for HR deficiency as assessed by "genomic scar" assays.[47-49] Our results suggests PARP inhibitors as a potential new treatment modality for the HR-deficient subgroup of endometrial cancer, which is further supported by a recently published case report in which a patient with EEC with a germline *BRCA2* variant (and a somatic hit of the wild-type allele) experienced a durable response to the PARP inhibitor olaparib.[50]

The performance of several candidate "HRD biomarkers" to predict therapy response are currently being studied, among which many that include the analysis of pathogenic variants in HR genes or the presence of *BRCA*-associated "genomic scars" in tumor DNA.[16, 21-23, 51] At this moment, it is still unknown which of the available HRD biomarkers is most powerful to predict therapy response. The HR status as determined by the RAD51 assay used in this study, has been shown to be strongly associated with achieving a complete pathologic response to neoadjuvant chemotherapy in patients with breast cancer,[26] could predict in vitro PARP-inhibitor cytotoxicity in primary cell cultures obtained from epithelial ovarian cancers,[52, 53] and could predict platinum sensitivity as well as improved survival outcome in patients with EOC

and HGSOC.[27, 53] Because the RAD51 assay is performed on fresh, irradiated tumor tissue, it currently has limited potential to be routinely used in clinical diagnostics, whereas methods that can assess "genomic scars" in FFPE-derived DNA are more suitable for this purpose.[51] Interestingly, in the recently published study of Cruz and colleagues, low levels of RAD51 foci in nonirradiated tumors correlated with PARP-inhibitor sensitivity in xenograft models.[54] When this approach can be validated on (archived) human FFPE-tumor tissue, the assessment of RAD51 to define HR status would become clinically feasible.

Our study is not without limitations. Our cohort is enriched for high-grade endometrial cancers cases, because we prospectively recruited patients in the LUMC, which is a referral center for endometrial cancer. Therefore, the prevalence of HR deficiency in our endometrial cancer cohort is likely an overestimate given the strong association with NEEC. Studies on larger cohorts are necessary to establish a more precise estimate of the prevalence of HR deficiency among the diverse endometrial cancer histotypes. Finally, the molecular analysis we performed was extensive, but not exhaustive. We used a targeted NGS panel and a aCGH/SNP array to identify the molecular cause of HR deficiency. In the future, whole-exome/genome sequencing may be preferred, not only to have the possibility to identify pathogenic variants in additional genes but also to explore the relationship between the outcome of the RAD51-assay and established genomic scars.

In conclusion, we are the first to demonstrate that HR is frequently abrogated in a subset of endometrial cancers, in particularly the "serous-like", *TP53*-mutated subclass of endometrial cancers, the group with the worst clinical outcome. This study provides a strong rationale for future clinical trials aiming to target HR-deficient high-grade endometrial cancers with therapies exploiting this defect, such as platinum compounds and PARP inhibitors.

Acknowledgements

The authors would thank E.M. Osse (LUMC), E.J. Dreef (LUMC) and M. Francilette (IGR) for their excellent technical assistance.

Grant support

This work was supported by The Dutch Cancer Society KWF-Alpe d'HuZes (grant EMCR: 2014-7048 to M.P.G. Vreeswijk). M.A. Glaire is funded by a Wellcome Trust Clinical Training Fellowship. D.N. Church is funded by an Academy of Medical Sciences / Health Foundation Clinician Scientist Fellowship. The research was funded/supported by the National Institute for Health Research (NIHR) Oxford Biomedical Research Centre (BRC). The views expressed are those of the author(s) and not necessarily those of the NHS, the NIHR or the Department of Health.

Disclosure of potential conflicts of interest

PCS's spouse is employed by AstraZeneca. No other potential conflicts of interest were disclosed.

References

1. Torre LA, Bray F, Siegel RL, Ferlay J, Lortet-Tieulent J, Jemal A. Global cancer statistics, 2012. CA Cancer J Clin 2015;65(2):87-108.
2. Colombo N, Creutzberg C, Querleu D, Barahona M, Sessa C, ESMO Guidelines Committee. Appendix 5: Endometrial cancer: eUpdate published online 8 June 2017 (www.esmo.org/Guidelines/Gynaecological-Cancers). Ann Oncol 2017;28(suppl_4):iv153-iv6.
3. Colombo N, Creutzberg C, Amant F, Bosse T, Gonzalez-Martin A, Ledermann J, et al. ESMO-ESGO-ESTRO Consensus Conference on Endometrial Cancer: Diagnosis, Treatment and Follow-up. Int J Gynecol Cancer 2016;26(1):2-30.
4. Hamilton CA, Cheung MK, Osann K, Chen L, Teng NN, Longacre TA, et al. Uterine papillary serous and clear cell carcinomas predict for poorer survival compared to grade 3 endometrioid corpus cancers. Br J Cancer 2006;94(5):642-6.
5. McGunigal M, Liu J, Kalir T, Chadha M, Gupta V. Survival Differences Among Uterine Papillary Serous, Clear Cell and Grade 3 Endometrioid Adenocarcinoma Endometrial Cancers: A National Cancer Database Analysis. Int J Gynecol Cancer 2017;27(1):85-92.
6. Bendifallah S, Canlorbe G, Collinet P, Arsene E, Huguet F, Coutant C, et al. Just how accurate are the major risk stratification systems for early-stage endometrial cancer? Br J Cancer 2015;112(5):793-801.
7. Kandoth C, Schultz N, Cherniack AD, Akbani R, Liu Y, Shen H, et al. Integrated genomic characterization of endometrial carcinoma. Nature 2013;497(7447):67-73.
8. Cherniack AD, Shen H, Walter V, Stewart C, Murray BA, Bowlby R, et al. Integrated Molecular Characterization of Uterine Carcinosarcoma. Cancer cell 2017;31(3):411-23.
9. Rosa-Rosa JM, Leskela S, Cristobal-Lana E, Santon A, Lopez-Garcia MA, Munoz G, et al. Molecular genetic heterogeneity in undifferentiated endometrial carcinomas. Mod Pathol 2016;Nov;29(11):1390-1398.
10. DeLair DF, Burke KA, Selenica P, Lim RS, Scott SN, Middha S, et al. The genetic landscape of endometrial clear cell carcinomas. J Pathol. 2017;243(2):230-241.
11. Stelloo E, Bosse T, Nout RA, MacKay HJ, Church DN, Nijman HW, et al. Refining prognosis and identifying targetable pathways for high-risk endometrial cancer; a TransPORTEC initiative. Mod Pathol 2015;28(6):836-44.
12. Talhouk A, McConechy MK, Leung S, Li-Chang HH, Kwon JS, Melnyk N, et al. A clinically applicable molecular-based classification for endometrial cancers. Br J Cancer 2015;113(2):299-310.
13. Stelloo E, Nout RA, Osse EM, Jurgenliemk-Schulz IJ, Jobsen JJ, Lutgens LC, et al. Improved Risk Assessment by Integrating Molecular and Clinicopathological Factors in Early-stage Endometrial Cancer-Combined Analysis of the PORTEC Cohorts. Clin Cancer Res 2016;22(16):4215-24.
14. Konstantinopoulos PA, Ceccaldi R, Shapiro GI, D'Andrea AD. Homologous Recombination Deficiency: Exploiting the Fundamental Vulnerability of Ovarian Cancer. Cancer Discov 2015;5(11):1137-54.
15. Lord CJ, Ashworth A. BRCAness revisited. Nat rev Cancer 2016;16(2):110-20.

16. Roy R, Chun J, Powell SN. BRCA1 and BRCA2: different roles in a common pathway of genome protection. Nat Rev Cancer 2012;12(1):68-78.
17. de Jonge MM, Mooyaart AL, Vreeswijk MP, de Kroon CD, van Wezel T, van Asperen CJ, et al. Linking uterine serous carcinoma to BRCA1/2-associated cancer syndrome: A meta-analysis and case report. Eur J Cancer 2017;72:215-25.
18. Shu CA, Pike MC, Jotwani AR, Friebel TM, Soslow RA, Levine DA, et al. Uterine Cancer After Risk-Reducing Salpingo-oophorectomy Without Hysterectomy in Women With BRCA Mutations. JAMA oncol 2016; 1;2(11):1434-1440.
19. Ring KL, Bruegl AS, Allen BA, Elkin EP, Singh N, Hartman AR, et al. Germline multi-gene hereditary cancer panel testing in an unselected endometrial cancer cohort. Mod Pathol 2016 Nov;29(11):1381-1389.
20. Shen WH, Balajee AS, Wang J, Wu H, Eng C, Pandolfi PP, et al. Essential role for nuclear PTEN in maintaining chromosomal integrity. Cell 2007;128(1):157-70.
21. Davies H, Glodzik D, Morganella S, Yates LR, Staaf J, Zou X, et al. HRDetect is a predictor of BRCA1 and BRCA2 deficiency based on mutational signatures. Nat Med 2017;23(4):517-525.
22. Abkevich V, Timms KM, Hennessy BT, Potter J, Carey MS, Meyer LA, et al. Patterns of genomic loss of heterozygosity predict homologous recombination repair defects in epithelial ovarian cancer. Br J Cancer 2012;107(10):1776-82.
23. Popova T, Manie E, Rieunier G, Caux-Moncoutier V, Tirapo C, Dubois T, et al. Ploidy and large-scale genomic instability consistently identify basal-like breast carcinomas with BRCA1/2 inactivation. Cancer Res 2012;72(21):5454-62.
24. Alexandrov LB, Nik-Zainal S, Wedge DC, Aparicio SA, Behjati S, Biankin AV, et al. Signatures of mutational processes in human cancer. Nature 2013;500(7463):415-21.
25. Naipal KA, Verkaik NS, Ameziane N, van Deurzen CH, Ter Brugge P, Meijers M, et al. Functional ex vivo assay to select homologous recombination-deficient breast tumors for PARP inhibitor treatment. Clin Cancer Res 2014;20(18):4816-26.
26. Graeser M, McCarthy A, Lord CJ, Savage K, Hills M, Salter J, et al. A marker of homologous recombination predicts pathologic complete response to neoadjuvant chemotherapy in primary breast cancer. Clin Cancer Res 2010;16(24):6159-68.
27. Tumiati M, Hietanen S, Hynninen J, Pietila E, Farkkila A, Kaipio K, et al. A functional homologous recombination assay predicts primary chemotherapy response and long-term survival in ovarian cancer patients. Clin Cancer Res 2018 24(18):4482-4493.
28. Willers H, Taghian AG, Luo CM, Treszezamsky A, Sgroi DC, Powell SN. Utility of DNA repair protein foci for the detection of putative BRCA1 pathway defects in breast cancer biopsies. Mol Cancer Res 2009;7(8):1304-9.
29. Buck SB, Bradford J, Gee KR, Agnew BJ, Clarke ST, Salic A. Detection of S-phase cell cycle progression using 5-ethynyl-2'-deoxyuridine incorporation with click chemistry, an alternative to using 5-bromo-2'-deoxyuridine antibodies. BioTechniques 2008;44(7):927-9.

30. van Eijk R, Stevens L, Morreau H, van Wezel T. Assessment of a fully automated high-throughput DNA extraction method from formalin-fixed, paraffin-embedded tissue for KRAS, and BRAF somatic mutation analysis. Exp Mol Pathol 2013;94(1):121-5.
31. Riaz N, Blecua P, Lim RS, Shen R, Higginson DS, Weinhold N, et al. Pan-cancer analysis of bi-allelic alterations in homologous recombination DNA repair genes. Nat Commun 2017;8(1):857.
32. Plon SE, Eccles DM, Easton D, Foulkes WD, Genuardi M, Greenblatt MS, et al. Sequence variant classification and reporting: recommendations for improving the interpretation of cancer susceptibility genetic test results. Hum Mutat 2008;29(11):1282-91.
33. Church DN, Stelloo E, Nout RA, Valtcheva N, Depreeuw J, ter Haar N, et al. Prognostic significance of POLE proofreading mutations in endometrial cancer. J Natl Cancer Inst 2015;107(1):402.
34. Broad Institute TCGA Genome Data Analysis Center (2016): Firehose 2016_01_28 run. Broad Institute of MIT and Harvard. doi:10.7908/C11G0KM9.
35. Schouten PC, Vis DJ, van Dijk E, Lips EH, Scheerman E, van Deurzen CHM, et al. Chapter 3: Copy number signatures of BRCA1 and BRCA2 association across breast and ovarian cancer. In: Schouten P.C. Identification and treatment of patients with BRCA1 or BRCA2-defective breast and ovarian cancer. Genes and mechanisms involved in malignant conversion. In: Harris CC, Liotta LA, editors. Genetic mechanisms in carcinogenesis and tumor progression. ProefschriftMaken; 2016 p. 95-132.
36. Rayner E, van Gool IC, Palles C, Kearsey SE, Bosse T, Tomlinson I, et al. A panoply of errors: polymerase proofreading domain mutations in cancer. Nat Rev Cancer 2016;16(2):71-81.
37. Norquist B, Wurz KA, Pennil CC, Garcia R, Gross J, Sakai W, et al. Secondary somatic mutations restoring BRCA1/2 predict chemotherapy resistance in hereditary ovarian carcinomas. J Clin Oncol 2011;29(22):3008-15.
38. Bian X, Gao J, Luo F, Rui C, Zheng T, Wang D, et al. PTEN deficiency sensitizes endometrioid endometrial cancer to compound PARP-PI3K inhibition but not PARP inhibition as monotherapy. Oncogene 2018;37(3):341-51.
39. Miyasaka A, Oda K, Ikeda Y, Wada-Hiraike O, Kashiyama T, Enomoto A, et al. Anti-tumor activity of olaparib, a poly (ADP-ribose) polymerase (PARP) inhibitor, in cultured endometrial carcinoma cells. BMC cancer 2014;14:179.
40. Mendes-Pereira AM, Martin SA, Brough R, McCarthy A, Taylor JR, Kim JS, et al. Synthetic lethal targeting of PTEN mutant cells with PARP inhibitors. EMBO Mol Med 2009;1(6-7):315-22.
41. Vollebergh MA, Lips EH, Nederlof PM, Wessels LF, Wesseling J, Vd Vijver MJ, et al. Genomic patterns resembling BRCA1- and BRCA2-mutated breast cancers predict benefit of intensified carboplatin-based chemotherapy. Breast cancer res BCR 2014;16(3):R47.
42. Pennington KP, Walsh T, Harrell MI, Lee MK, Pennil CC, Rendi MH, et al. Germline and somatic mutations in homologous recombination genes predict platinum response and survival in ovarian, fallopian tube, and peritoneal carcinomas. Clin Cancer Res 2014;20(3):764-75.
43. de Boer SM, Powell ME, Mileshkin L, Katsaros D, Bessette P, Haie-Meder C, et al. Adjuvant chemoradiotherapy versus radiotherapy alone for women with high-risk endometrial cancer (PORTEC-3): final results of an international, open-label, multicentre, randomised, phase 3 trial. Lancet Oncol 2018;19(3):295-309.

44. McMeekin DS, Filiaci VL, Thigpen JT, Gallion HH, Fleming GF, Rodgers WH. The relationship between histology and outcome in advanced and recurrent endometrial cancer patients participating in first-line chemotherapy trials: a Gynecologic Oncology Group study. Gynecol Oncol 2007;106(1):16-22.
45. Hogberg T, Signorelli M, de Oliveira CF, Fossati R, Lissoni AA, Sorbe B, et al. Sequential adjuvant chemotherapy and radiotherapy in endometrial cancer—results from two randomised studies. Eur J Cancer 2010;46(13):2422-31.
46. Gilks CB, Oliva E, Soslow RA. Poor interobserver reproducibility in the diagnosis of high-grade endometrial carcinoma. Am J Surg Pathol 2013;37(6):874-81.
47. Mirza MR, Monk BJ, Herrstedt J, Oza AM, Mahner S, Redondo A, et al. Niraparib Maintenance Therapy in Platinum-Sensitive, Recurrent Ovarian Cancer. N Engl J Med 2016;375(22):2154-64.
48. Ledermann J, Harter P, Gourley C, Friedlander M, Vergote I, Rustin G, et al. Olaparib maintenance therapy in patients with platinum-sensitive relapsed serous ovarian cancer: a preplanned retrospective analysis of outcomes by BRCA status in a randomised phase 2 trial. Lancet Oncol 2014;15(8):852-61.
49. Swisher EM, Lin KK, Oza AM, Scott CL, Giordano H, Sun J, et al. Rucaparib in relapsed, platinum-sensitive high-grade ovarian carcinoma (ARIEL2 Part 1): an international, multicentre, open-label, phase 2 trial. Lancet Oncol 2017;18(1):75-87.
50. Gockley AA, Kolin DL, Awtrey CS, Lindeman NI, Matulonis UA, Konstantinopoulos PA. Durable response in a woman with recurrent low-grade endometrioid endometrial cancer and a germline BRCA2 mutation treated with a PARP inhibitor. Gynecol Oncol 2018;150(2):219-226.
51. Hoppe MM, Sundar R, Tan DSP, Jeyasekharan AD. Biomarkers for Homologous Recombination Deficiency in Cancer. J Natl Cancer Inst 2018; 110(7):704-713.
52. Mukhopadhyay A, Elattar A, Cerbinskaite A, Wilkinson SJ, Drew Y, Kyle S, et al. Development of a functional assay for homologous recombination status in primary cultures of epithelial ovarian tumor and correlation with sensitivity to poly(ADP-ribose) polymerase inhibitors. Clin Cancer Res 2010;16(8):2344-51.
53. Mukhopadhyay A, Plummer ER, Elattar A, Soohoo S, Uzir B, Quinn JE, et al. Clinicopathological features of homologous recombination-deficient epithelial ovarian cancers: sensitivity to PARP inhibitors, platinum, and survival. Cancer Res 2012;72(22):5675-82.
54. Cruz C, Castroviejo-Bermejo M, Gutierrez-Enriquez S, Llop-Guevara A, Ibrahim YH, Gris-Oliver A, et al. RAD51 foci as a functional biomarker of homologous recombination repair and PARP inhibitor resistance in germline BRCA mutated breast cancer. Ann Oncol 2018; 29(5):1203-1210.

Supplementary materials and methods

Immunofluorescence staining

Sections of 5 µm were used. After deparaffinization in xylene and rehydration in ethanol, target antigen retrieval was performed using DAKO Antigen Retrieval buffer (pH 9.0) at 97°C for 12 minutes using a TissueWave™ 2 Microwave Processor (Thermo Scientific). Cells were permeabilized with a mixture of 0,2% Triton X-100 in phosphate buffered saline (PBS) for 20 minutes, followed by 1 hour incubation at 37°C with DNase (10.000 U/ml, dilution 1/10 in PBS, Roche diagnostics). Blocking was achieved using PBS with 2% FBS and 1% bovine serum albumin (BSA) for 30 minutes at room temperature. Sections were co-stained for RAD51 and Geminin with the primary antibodies (anti-RAD51 (GTX70230, 1/400, GeneTex) and anti-geminin (10802-1-AP, 1/400, Protein Tech group), diluted in blocking buffer) and incubated for 1 hour at room temperature. The secondary antibodies for visualizing the primary antibodies were Alexa Fluor 555 (A21424, 1/1000, Life Technologies) and Alexa Fluor 488 (A11034, 1/1000, Life Technologies), both diluted in blocking buffer. For EdU detection, the Click-iT® reaction cocktail was prepared according to manufacturer's instructions, with Alexa Fluor 647 (cat. C10340, 1/1000, life technologies) for visualization. The tissue sections were incubated for 30 minutes at room temperature with the EdU cocktail mix. Lastly, the tissue sections were mounted with Vectashield ProLong Antifade Mountant with DAPI (Thermofisher Scientific, cat. p36934).

aCGH

For each sample in the Agilent aCGH analysis cohort, DNA was restriction digested and controlled by Agilent Bioanalyzer on DNA 7500 chips (Agilent Technologies, Santa Clara, CA, USA) and labelled with Cy3-dUTP or Cy5-dUTP using Agilent Genomic DNA Labelling Kit PLUS. Hybridization was carried out on Agilent 4x180kb arrays for 24 hours at 65°C in a rotating oven (Robbins Scientific, Mountain View, CA) at 20 rpm, according to the manufacturer's instructions. A commercial DNA was used for control (Promega). Scanning was performed with an Agilent G2505C DNA Microarray scanner using default parameters. Quantification of Cy5 and Cy3 signals from scans was performed with Feature Extraction v10.5.1.1 (Agilent Technologies) using default parameters. Resulting raw signals and log2 (ratio) profiles were normalized and centered according to their dye composition (Cy5/Cy3) and local GC content. These profiles were segmented with the Circular Binary Segmentation algorithm through its implementation in the DNA copy package for R v(v2.6 to v3.1) using default parameters. DNA copy number imbalances were detected considering a minimum of 3 consecutive probes and a minimal absolute amplitude threshold that was specific for each profile. Profiles were centered using the most centered out of the three most populated peaks of the smoothed log2(Test/Ref) distribution. Aberration levels were called by setting a log2(Test/Ref) threshold automatically adapted to the internal noise for each profile, considered as one-fourth of the median value of the absolute differences between consecutive log2(Test/Ref) measures

along the genome. All genomics coordinates were established using the human genome as defined by the UCSC build hg19 (GRCh37). The copy number alterations detected with aCGH were transformed into log2 ratio.

SNP array

The experimental procedure of the OncoScan™ FFPE Assay Kit (335k probes, Thermo Fisher) includes several steps. Probes were added to the sample DNA (80ng as previously stated), and allowed to anneal at 58°C overnight (16–18 h) subsequent to an initial denaturation (95°C for 5 min). Samples were then split into two separate reactions, and proceeded as follows: dATP (A) and dTTP (T) (A/T) were added to one reaction, and dGTP (G) and dCTP (C) (G/C) were added to the second in order to conduct gap fill.

Unincorporated and non-circularized Molecular Inversion Probes (MIP), as well as the remains of the genomic template, were removed by treatment with exonucleases (Affymetrix, Inc.). The circular MIPs that were gap-filled by the A/T or G/C nucleotides were cleaved and their linear form was amplified by PCR. Subsequently, the 120-bp PCR product was cut and the smaller (44-bp) fragment containing the specific SNP genotype was subjected for hybridization onto array. Prior to this, samples were mixed with hybridization buffer and injected into the cartridges for 16–18 h at 49°C and 0.013 × g. Following hybridization, cartridges were removed from the oven, and stained using the GeneChip® Fluidics Station 450 (Affymetrix, Inc.), according to the manufacturer's protocol. Subsequent to staining and washing, arrays were scanned in GeneChip Scanner and the fluorescence of clusters was measured in order to generate a DAT file. Cluster intensities values were automatically calculated using built-in algorithm from DAT files by the Affymetrix GeneChip Command Console software, version 4.0 (Affymetrix, Inc.), and output in a CEL file format was created.

Raw probes intensities were aggregated to probesets and normalized using Affymetrix Power Tools v1.18.2. Normalized Log2Ratio, B-Allele Frequency (BAF) and metadata were extracted from the resulting OSCHP files. The Log2Ratio obtained then went through an additional renormalization step according to local GC-content, and centered as described in the aCGH paragraph. The R ASCAT package (v2.4.2) was then used in order to co-segment Log2Ratio and BAF values and to derive Allele-Specific Copy Number (ASCN) and Total Copy Number (TCN), using the maximal "goodness of fit" criterion to select the optimal ASCN model. This process has been developed in Gustave Roussy and is referred to as "EaCoN" (will be further published).

Genomic instabilisty score (GIS)

We created a software called getStability.py that takes as input a .CBS file and uses a cytoband file from the UCSC in order to classify events in the following classes based on segment lengths (with a 5% tolerance):

1. Whole Chromosome Event
2. Arm + event (which is defined as an event that is greater than one chromosomal arm, but lower than a chromosomal event)
3. Arm event
4. Greater than 30Mb and lower than a whole chromosome arm
5. Between 30Mb and 15Mb event
6. Between 15Mb and 1Mb event
7. Lower than 1Mb event

Based on these results, we summed up the events from classes 4 and 5 and called this result the genomic instability score. Using this instability score, we were able to classify samples in three classes using k-means (python package sklearn, 3 clusters, 2000 iterations, all other parameters set to default).

```
#K-Means analysis
import sklearn.cluster
import numpy as np
import pandas as pd
# Text file containing sample names & Scores
#1) Simple data transformation
a = open('AUAU_cohort', 'r').readlines()
b = [x.rstrip('\n').split('\t') for x in a]
c = [(x[0], int(x[1]), int(x[1])) for x in b]
f = np.array([(x[1], x[1]) for x in c])
#2) Put data in an pandas dataframe so we can keep sample names in (cannot do that with numpy)
g = pd.DataFrame(f, index=[x[0] for x in c])
#3) Prepare the classifier
classifier = sklearn.cluster.KMeans(n_clusters=3, max_iter=2000)
#4) Fit on the classifier
p = classifier.fit(g)
#5) Fill the pandas dataframe with the results from the classifier.
g.assign(rank=p.labels_)
```

Next generation sequencing

Library preparation and target enrichment was performed using the Sureselect$^{XT\ HS}$ Target Enrichment System for Illumina Paired-End Multiplexed Sequencing library reagent kit (Agilent technologies, Santa Clara, California, United States) according to manufacturer's instructions, with manual preparation of 16 sample sets. The captured DNA libraries were sequenced (16 samples per run) using the Illumina MiSeq (Illumina, San Diego, California, United States). The average depth of sequencing was 300X to assure a limit of detection of at least around 5% and a coverage of at least 90% at 200X and 100% at 100X.

The data analysis pipeline included the following algorithms: BWA-MEM v-0.7.12 for read alignment to the hg19 human reference genome and Samtools v-1.2 and Picard-tools v-1.139 for PCR duplicate quantification and removal. GATK Haplotype v-3.4-46, snpEff v-4.0 and MutaCaller-1.7 (home pileup internally developed) were used for variant calling and classification. Variants were called with a minimum allelic frequency threshold of 1% for already classified variants (those known in the internal database) and 5% for non-classified variants, and a read depth threshold of 30X for the total reads at the variant location and at least 10X for the variant.

Several filters were applied to further select for potential relevant variants among the called variants. The population databases Exac and gnomAd were used to automatically filter out polymorphism as soon as the population frequency was higher than 0.5%. Non-classified variants (not known in the internal database) were excluded if the intrarun recurrency within the 16 analyzed samples per illumina run was superior to 4/16 (25%), as this may be an indicator for an artefact or polymorphism.

Variants were categorized using the five-tier pathogenicity classification according to Plon et al., 2008; class 1=benign, class 2=likely benign, class 3=variant of unknown significance (VUS), class 4=likely pathogenic, class 5=pathogenic.[1] An internal database for germline *BRCA1/2* mutations comprising 15 years of sequencing experience in the French population, combined with the data of the UMD-BRCAshare *BRCA1/2* database (www.umd.be/BRCA1/ and www.umd.be/BRCA2/) was used to assign pathogenicity to detected variants. For non-BRCA1/2 alterations, all variants leading to a premature stop codon were considered as deleterious. Additionally, public databases as ClinVar (selection for the three stars curated data only) were applied for variant classification. All missense variants for which no functional data was present were considered as unclassified (class 3).

The presence of all but one pathogenic variant in HR genes, and the *RAD51D* VUS in Case 36 (Supplementary Table S3), were confirmed by bi-directional Sanger sequencing (details of PCR primers and reaction conditions available upon request). The *CHEK2* c.1510G>T variant located in exon 14 could not be confirmed. This region is known to share high homology with several pseudogenes which reduces the sensitivity to identify the variant at low VAF.[2]

The presence of loss of heterozygosity of the wildtype allele (LOH) was assessed based on the variant allele frequency of both the HR gene variants and single nucleotide polymorphisms (SNPs), in combination with the tumor percentage. LOH was considered to be present when the tumor cell percentage was >20%, the HR variant allele frequency was >60%, and/or at least two informative SNPs showed a variant allele frequency of <0.4 or >0.6. Absence of LOH could not be assessed with certainty for the variants with an allelic frequency of <50% due to the possibility of subclonality.

BRCA1-promoter hypermethylation

Approximately 75 ng of FFPE-isolated DNA was denatured for 5 minutes at 98°C and subsequently cooled down to 25°C. After addition of the SALSA probe-mix and MLPA-buffer, samples were incubated for 1 minute at 98°C, followed by hybridization at 60°C for 16-20 hours. Next, ligasebuffer A was added and samples were heated to 48°C. Samples were then split and ligated (ligasebuffer B and Ligase-65 enzyme) with or without the addition of HhaI-enzyme for 30 minutes at 48°C followed by heating for 5 minutes at 98°C. Then, the PCR-mastermix (including SALSA primermix and SALSA polymerase) was added and the following PCR reaction was performed for 35 cycles; 30 seconds at 95°C, 30 seconds at 60°C and 60 seconds at 72°C, followed by an incubation period for 20 minutes at 72°C. The amplified PCR products were separated by electrophoresis on an ABI 3130 genetic analyzer (Applied Biosystems) and analyzed using Coffalyser.Net software (MRC-Holland).

IHC staining

For manually stained sections, following deparaffinization in xylene and rehydration via a graded ethanol series, blockage of the endogenic peroxidase activity (0,3% Methanol/H_2O_2) was performed. Antigen retrieval was achieved using a microwave oven procedure for 10 minutes in 10 mmol/L Tris-EDTA buffer, pH9.0 (MSH6 and PMS2) or in a 10mmol/L citrate buffer, pH 6.0 (PTEN and MRE11). Sections were incubated overnight with antibodies at room temperature (PTEN, MSH6 and MRE11) or at 4°C (PMS2). The sections were then incubated for 30 minutes using a secondary antibody (Poly-HRP-GAM/R/R; DPV0110HRP; ImmunoLogic). For PMS2 and MSH6, before incubation with the secondary antibody, an additional 15 minute incubation step with a linker (EnVision FLEX+ rabbit, SM805, DAKO) was performed. As chromogen, DAB+ (K3468, DAKO) was used. The slides were counterstained with haematoxylin. For the automated stainer standard protocols and the same IHC-clones were used with some slight differences. An additional linker was used for PMS2- and BAP1-stainings and not for MSH6. All BAP1 slides were stained using an automated stainer. As secondary antibody and chromogen we respectively used EnVision™ FLEX /HRP (Dako SM802) and EnVision™ FLEX DAB+ Chromogen (Dako DM827) diluted in EnVision™ FLEX Substrate Buffer (Dako SM803).

IHC scoring

All slides were evaluated by two observers, blinded for patient characteristics and outcome of the functional RAD51 assay.

To assign MMR status, PMS2- and MSH6-IHC expression were scored in three categories as described previously by Stelloo and colleagues; retained, loss and subclonal/regional loss of protein expression.[3] Subclonal/regional loss was defined as a tumor with retained nuclear expression showing focal loss of nuclear expression in a discrete tumour area of at least 10% of the total tumor volume, with positive staining of stromal cells/infiltrate as

an internal control. Tumors in which at least one of the mismatch repair proteins showed loss of expression were considered MMR-deficient (MMRd). Subclonal loss was considered partial MMRd.[3] PTEN staining was evaluated in three categories as described before; negative, positive and heterogeneous.[4] Heterogeneous cases were further subdivided in diffuse patchy staining (considered positive) and subclonal/regional; negative except for a well demarcated area (considered negative). MRE11 expression was scored as negative (no nuclear staining) or positive (weak, moderate or strong nuclear staining). BAP1 expression was scored as positive (nuclear staining) or negative (no nuclear staining).

TCGA classification based on surrogate markers

The EC were classified in previously described molecular subclasses using the following surrogate markers; pathogenic *TP53* variants for SCNA-hi/*TP53*-mutated, *POLE* mutations for *POLE/*ultramutated and mismatch repair(MMR)-IHC (PMS2, MSH6) for MMR-deficient (MMRd)/hypermutated. All ECs without classifying features were classified as SCNA-low/no specific molecular profile (NSMP). Cases with more than one classifying feature were assigned as follows; *POLE/TP53*-mutation to *POLE/*ultramutated, MMRd/*TP53* and MMRd/*POLE* to MMRd/hypermuted, unless the MMR expression loss was subclonal.

Genomic signatures TCGA cohort

- ***BRCA-like* profiles**

Shrunken centroids classifiers were previously trained on a training cohort of 73 ovarian cancer and 110 breast cancer patients to distinguish aCGH copy number profiles of *BRCA1* mutated breast and ovarian cancer cases from control cases and *BRCA2* mutated breast and ovarian cancer cases from control cases.[5] Area under the receiver/operator curves were respectively 0.72 and 0.67. These were subsequently independently validated in the validation cohort consisting of TCGA breast and ovarian cancers. Analyses were combined since the classifier was trained on both tumor types. 86% of the *BRCA1* mutated and methylated breast and ovarian cancers were correctly identified, and 61% of the *BRCA2* mutated breast and ovarian cancers.[5] Although slightly better performance was obtained when analysing tumor types separately, a combined breast and ovarian classifier was hypothesised to perform better in endometrial cancer as tumor type specific aberrations might be smoothed out. We processed the EC TCGA data to have a similar mean and range of values and subsequently applied before mentioned classifiers to this dataset. The classifier assigns a probability of having similar gains and losses as *BRCA* mutated cases ranging between 0 (similar to non-mutated cases) and 1 (similar to mutated cases). A cutoff of 0.5 of the posterior probability was used, as this is a two-class problem in which errors for both classes were considered equally important.

- ***Large-scale state transitions (LST), COSMIC Signature 3 and bi-allelic alterations in HR genes***

Somatic mutation annotation files (MAF), relevant as of 28th January 2016, for individual cancers as part of the TCGA were obtained from Firebrowse (http://firebrowse.org/).[6] EC (UCEC) tumors were classified according to the presence of bi-allelic pathogenic mutation in the 102 homologous recombination genes defined by Riaz and colleagues.[7] Affymetrix SNP Array 6.0 (SNP6) array data was obtained from Firebrowse (http://firebrowse.org/), dated 28th January 2016. To asses for genomic features of genomic instability, the number of large-scale state transitions (LST) was determined for each cancer following methods detailed by Riaz and colleagues,[7] and using the same cut-off to define HR deficiency status (≥15). The proportion of mutations in each endometrial cancer case that were similar to the signatures described by Alexandrov and colleagues,[8] were determined by non-negative least squares regression and had been provided in the supplementary data from Riaz and colleagues.[7] The signature responsible for the majority of the mutations was defined as the dominant signature in that specific cancer. Signature 3 previously has been identified as being associated with *BRCA1* and *BRCA2* mutations.[8] These data were compiled in a matrix for the 541 EC in the TCGA data set.

References

1. Plon SE, Eccles DM, Easton D, Foulkes WD, Genuardi M, Greenblatt MS, et al. Sequence variant classification and reporting: recommendations for improving the interpretation of cancer susceptibility genetic test results. Hum Mutat 2008;29(11):1282-91.
2. Sodha N, Williams R, Mangion J, Bullock SL, Yuille MR, Eeles RA. Screening hCHK2 for mutations. Science (New York, NY) 2000;289(5478):359.
3. Stelloo E, Jansen AML, Osse EM, Nout RA, Creutzberg CL, Ruano D, et al. Practical guidance for mismatch repair-deficiency testing in endometrial cancer. Ann Oncol 2017;28(1):96-102.
4. Garg K, Broaddus RR, Soslow RA, Urbauer DL, Levine DA, Djordjevic B. Pathologic scoring of PTEN immunohistochemistry in endometrial carcinoma is highly reproducible. Int J Gynecol Pathol 2012;31(1):48-56.
5. Schouten PC, Vis DJ, van Dijk E, Lips EH, Scheerman E, van Deurzen CHM, et al. Chapter 3: Copy number signatures of BRCA1 and BRCA2 association across breast and ovarian cancer. In: Schouten P.C. Identification and treatment of patients with BRCA1 or BRCA2-defective breast and ovarian cancer. Genes and mechanisms involved in malignant conversion. In: Harris CC, Liotta LA, editors. Genetic mechanisms in carcinogenesis and tumor progression. ProefschriftMaken; 2016 p. 95-132.
6. Broad Institute TCGA Genome Data Analysis Center (2016): Firehose 2016_01_28 run. Broad Institute of MIT and Harvard. doi:10.7908/C11G0KM9.
7. Riaz N, Blecua P, Lim RS, Shen R, Higginson DS, Weinhold N, et al. Pan-cancer analysis of bi-allelic alterations in homologous recombination DNA repair genes. Nat Commun 2017;8(1):857.
8. Alexandrov LB, Nik-Zainal S, Wedge DC, Aparicio SA, Behjati S, Biankin AV, et al. Signatures of mutational processes in human cancer. Nature 2013;500(7463):415-21.

Supplementary tables and figures

Supplementary Table S1. Clinicopathological characteristics of the cases included in final analysis

	No	%
Total	25	100
Age, years		
Mean (SD)	67,4 ± 9,8	
Tumor		
Primary	24	96
Recurrent	1	4
Histologic subtype		
Endometrioid	12	48
Non-endometrioid	13	52
Serous	*4*	*16*
Carcinosarcoma, serous	*4*	*16*
Carcinosarcoma, endometrioid	*1*	*4*
Clear cell	*2*	*8*
Dedifferentiated	*2*	*8*
Histologic grade		
1	9	36
2	1	4
3	15	60
FIGO 2009		
I	18	72
II	0	0
III	3	12
IV	4	16
Ovarian/tubal involvement		
yes	4	16
no	21	84
Neoadjuvant treatment		
Yes	1	4
No	24	96

Supplementary Table S2. Clinicopathological characteristics of the homologous recombination intermediate cases

	HR intermediate
	n
Total	2
Age, years	
Mean ± SD	69 ±2.1
Tumor	
Primary	1
Recurrent	1
Histologic subtype	
Endometrioid	1
Non-endometrioid	1
Serous	*0*
Carcinosarcoma	*1*
Clear cell	*0*
Dedifferentiated	*0*
Histologic grade	
1+2	0
3	2
FIGO 2009	
I	1
III/IV	1
Adnexal involvement	
yes	1
no	1
PTEN-IHC	
loss of expression	2
normal expression	0
aCGH	
Copy Number extremely high	0
Copy number High	1
Copy number Low	1
TP53	
Mutation	0
No mutation	2
TCGA subgroup	
TP53	0
NSMP/*POLE*/MMRd	2

Abbreviations: HR, homologous recombination; MMRd, mismatch repair deficient; NSMP, no specific molecular profile.

Supplementary Table S3. **Overview of the detected class 3, 4 and 5 variants in the final cohort**

Case-ID	HR status	HR core	HR related	Other	c.DNA change	Amino Acid change	T%	VAF	variant class
01	**proficient**			*TP53*	c.742C>T	p.Arg248Trp	70	78%	class 5
03	**proficient**			*TP53*	c.638G>A	p.Arg213Glu	80	25%	class 5
				TP53	c.742C>T	p.Arg248Trp		28%	class 5
06	**proficient**						50		
07	**proficient**						60		
09	**deficient**	*BRCA1*			c.4327C>T	p.Arg1443*	70	94%	class 5
				TP53	c.659A>G	p.Tyr220Cys		38%	class 5
				TP53	c.742C>T	p.Arg248Trp		41%	class 5
12	**deficient**			*TP53*	c.396G>T	p.Lys132Asn	80	94%	Class 5
13	**deficient**			*TP53*	c.838A>G	p.Arg280Gly	80	95%	class 4
14	**proficient**						50		
15	**deficient**	*BRCA1*			c.3013delG	p.Glu1005fs	70	60%	class 5
				TP53	c.1009C>T	p.Arg337Cys		61%	class 5
16	**proficient**						60		
17	**proficient**						30		
18	**intermediate**	*BRIP1*			c.632delC	p.Pro211fs	70	28%	class 5
19	**deficient**		*ATM*		c.6543G>T	p.Glu2181Asp	70	34%	class 3
				TP53	c.581T>G	p.Leu194Arg		98%	class 4
20	**proficient**						70		
21	**proficient**			*TP53*	c.844C>T	p.Arg282Trp	80	49%	class 5
				TP53	c.919+1G>A	p.?		21%	class 5
22	**proficient**						70		
24	**proficient**			*TP53*	c.993+3A>T	p.?	80	34%	class 4
25	**proficient**						70		
26	**proficient**		*CHEK2*		c.1510G>T	p.Glu504*	60	28%	class 5
				TP53	c.523C>T	p.Arg175Cys		34%	class 4
				POLE	c.857C>G	p.Pro286Arg			class 4
27	**intermediate**	*BRCA2*			c.6373dupA	p.Thr2125fs	80	64%	class 5
		BRCA2			c.6306_6413del	p.Ser2103_Val2138del		28%	reverse
		BRIP1			c.2728G>T	p.Glu910*		39%	class 5
			CDK12		c.2813C>A	p.Ala938Asp		36%	class 3
29	**proficient**						50		
32	**proficient**		*ATM*		c.640delT	p.Ser214fs	75	5,5%	class 5
			ATM		c.7282A>G	p.Arg2428Gly		12%	class 3
			ATM		c.6583C>T	p.His2195Tyr		5,3%	class 3
			ATM		c.5846C>T	p.Ala1949Val		26%	class 3
				MMRd[a]					
33	**proficient**			*TP53*	c.491_520del	p.Lys164_Val173del	70	24%	class 5
34	**proficient**			*TP53*	c.659A>G	p.Tyr220Cys	90	93%	class 5
36	**deficient**	*RAD51D*			c.433C>T	p.Arg145Cys	75	32%	class 3
				TP53	c.818G>A	p.Arg273His		55%	class 5

Variants were annotated using build: hg19/GRCh37 and the following transcripts: *ATM,* NM_000051.3*; BRCA1,* NM_007294.3; *BRCA2,* NM_000059.3*; BRIP1,* NM_032043.2; *CDK12*, NM_016507.3; *CHEK2,* NM_007194.3*; POLE,* NM_006231.3*; RAD51D,* NM_002878.3; *TP53,* NM_000546.5.

[a]MMRd based on loss of PMS2 expression in immunohistochemistry.

Abbreviations: HR: Homologous recombination, MMRd: Mismatch repair-deficient, T%: tumor percentage, VAF: variant allele frequency

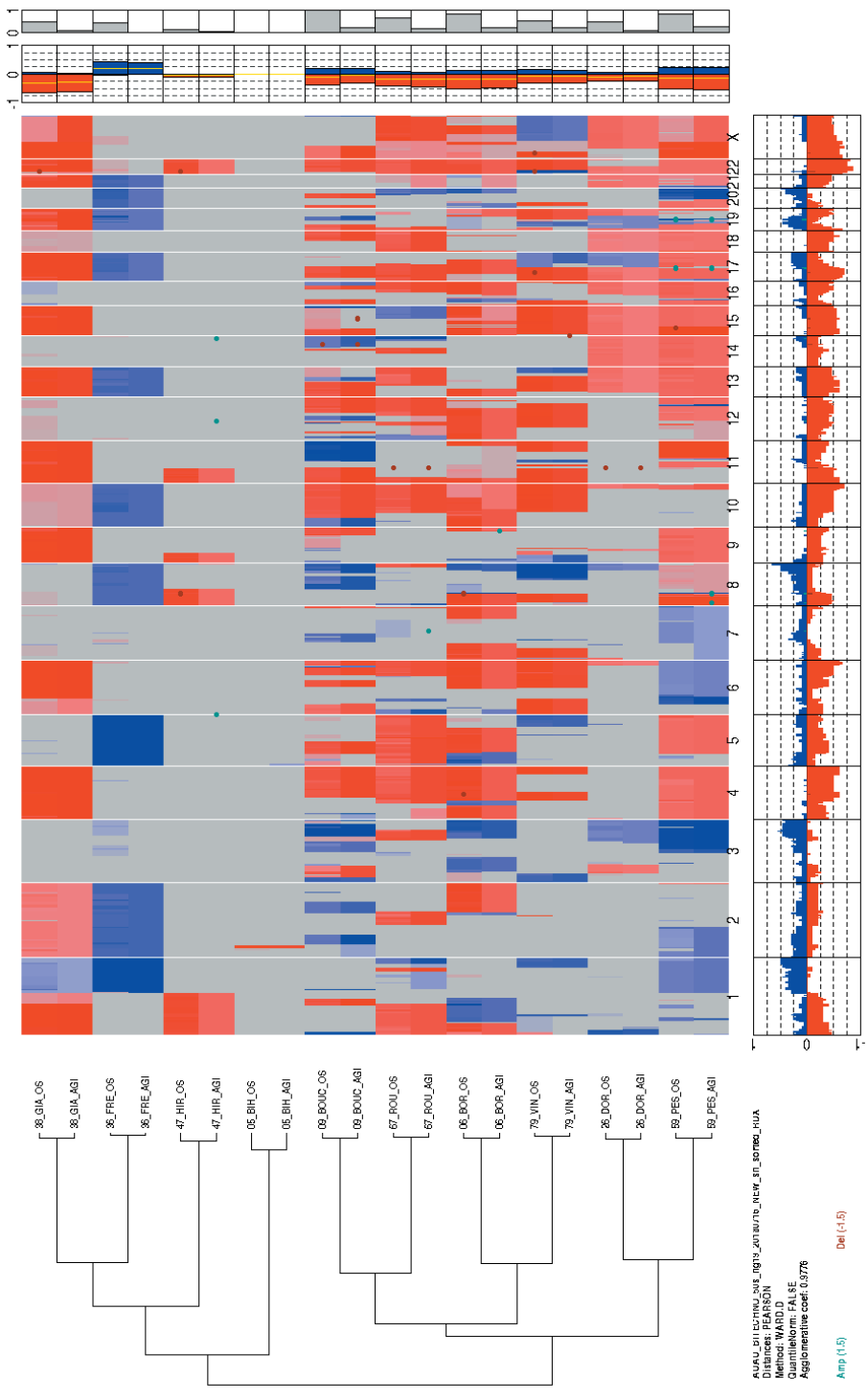

Supplementary Figure S1: Unsupervised Euclidean hierarchical clustering on ten paired FFPE and frozen ovarian cancer samples analysed respectively by Oncoscan (OS) or CGH Agilent (AGI) platforms. The figure shows perfect match between paired samples independently from their processing (OS or AGI).

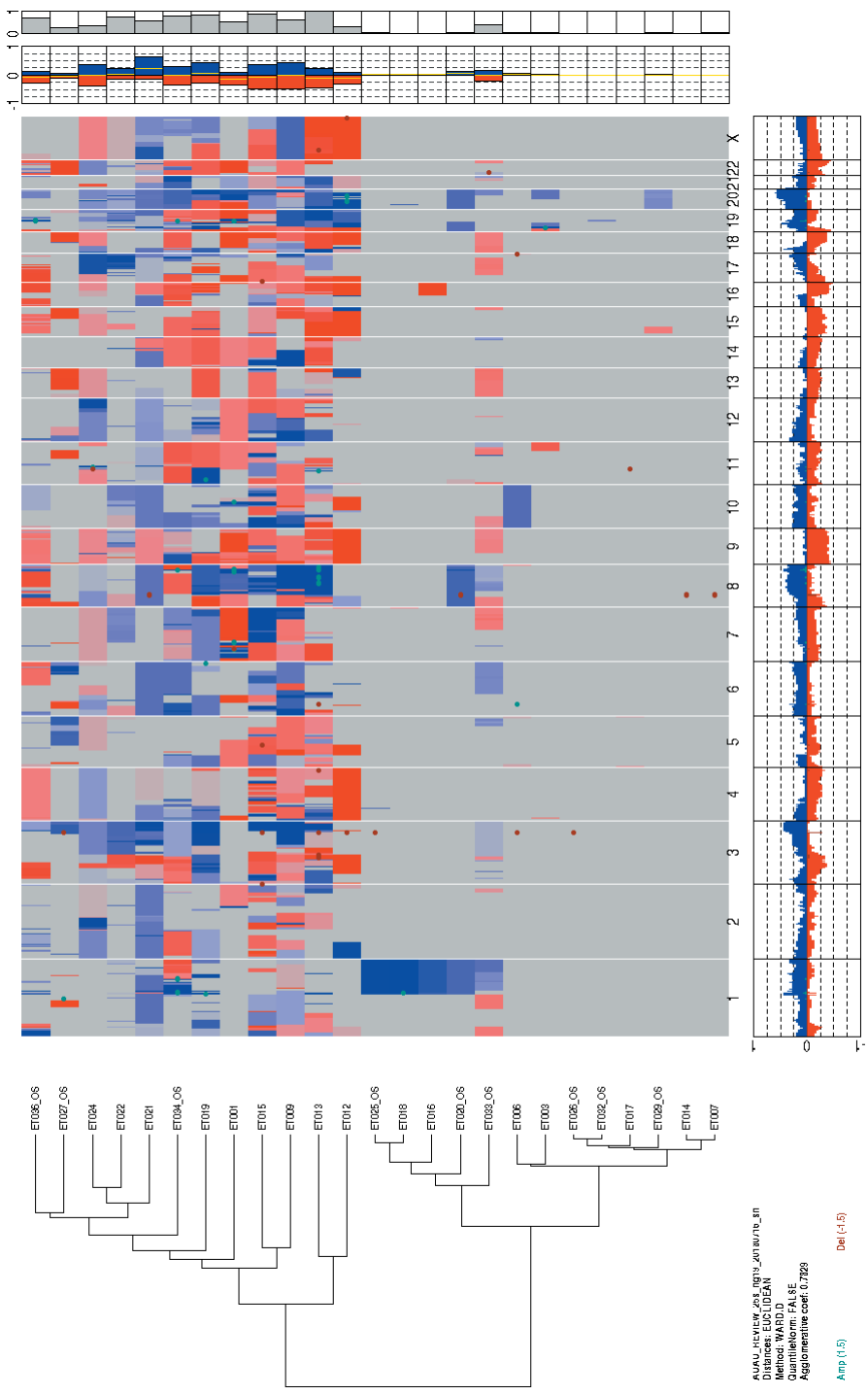

Supplementary Figure S2: Unsupervised Pearson hierarchical clustering on the endometrial cancer samples included in our paper. Samples labelled with "_OS" are those analysed by ONCOSCAN platform, others have been analysed using CGH Agilent technology. As can be seen, there is an unbiased natural division between samples.